Supplementary Information

Single-molecule two- and three-colour FRET studies reveal a transition state in SNARE disassembly by NSF

Sudheer K. Cheppali[1*], Chang Li[1*], Wenjing Xing[1*], Ruirui Sun[1], Mengyi Yang[1], Yi Xue[2], Si-Yao Lu[3], Jun Yao[3], Shan Sun[1†], Chunlai Chen[1†], Sen-Fang Sui[1,4†]

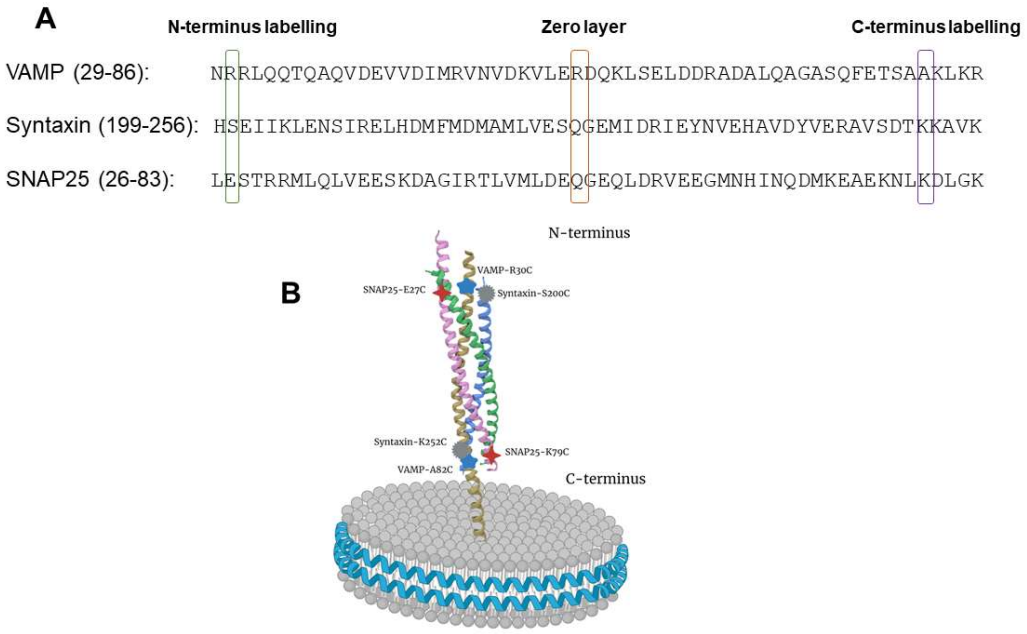

Supplementary Fig. 1. A) Sequence alignment and B) pictorial representation of labeled positions and labelled residues of SNARE proteins used in this study. B is created in BioRender. Cheppali, S. (2024) https://BioRender.com/k91i311.

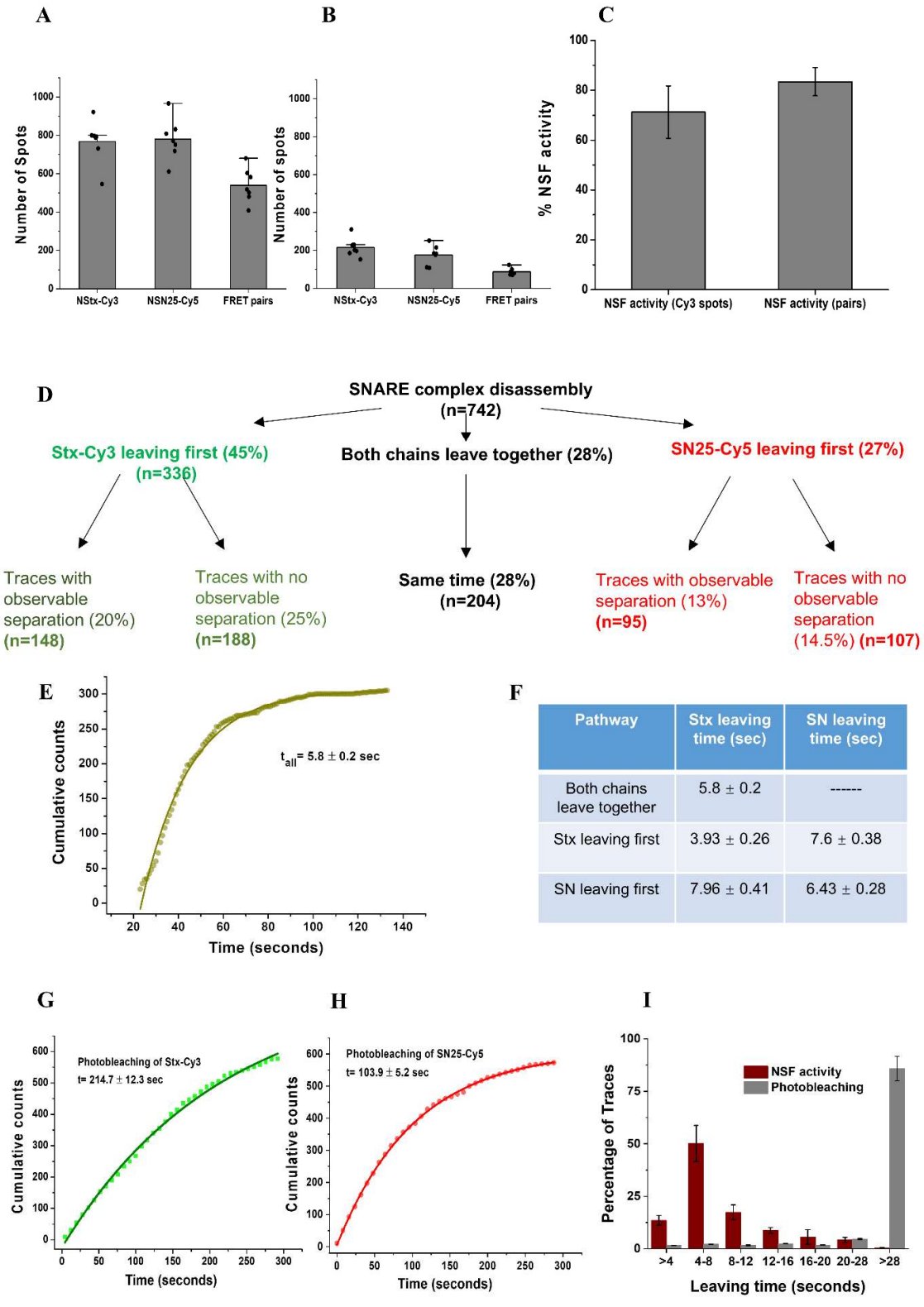

Supplementary Fig. 2. SNARE disassembly by NSF monitored using two-colour single-

molecule FRET. A) Number of NStx-Cy3 spots, NSN-Cy5 spots nd NStx-NSN25 FRET pairs observed after immobilization of SNARE nanodiscs on the TIRFM surface (t=0 sec). **B**) Number of NStx-Cy3 spots, NSN25-Cy5 spots and NStx-SN25 FRET pairs observed after the addition of α-SNAP, NSF along with 2 mM ATP and 2 mM $MgCl_2$ (t=200 sec) (n=8, independent SNARE disassembly experiments). **C**) Percent NSF activity based on the Cy3 spots and FRET pairs from **A** and **B,** errors are statistical. **D**) Classification of single-molecule trajectories based on the individual chain leaving (disassembly) time and also observable difference in the FRET and chain leaving separately. **E**) Cumulated distribution showing average chain leaving time when all the chains leave at the same time. **F**) Chain leaving times of various classes of traces observed as shown in Fig S1D. **G, H**) Graphs showing cumulative distribution of latencies for the photobleaching of NStx-Cy3 and NSN-Cy5, respectively, in the presence of oxygen scavenging buffer. **I**) Graph showing comparative chain leaving times of SNARE disassembly by NSF and photobleaching (n>500 traces in each case).

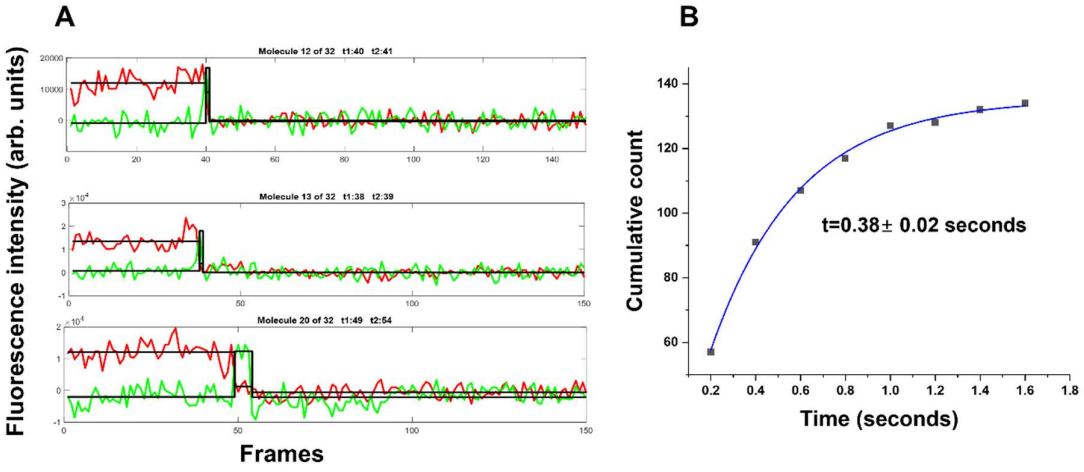

Supplementary Fig. 3. Hidden-Markov analysis of zero-FRET transient state. A) Two-color FRET example traces showing a separated zero-FRET state between NStx before its disassembly. **B**) Cumulative distribution of the transient NStx-Cy3 separated state before its disassembly showing its dwell time (n=138 traces).

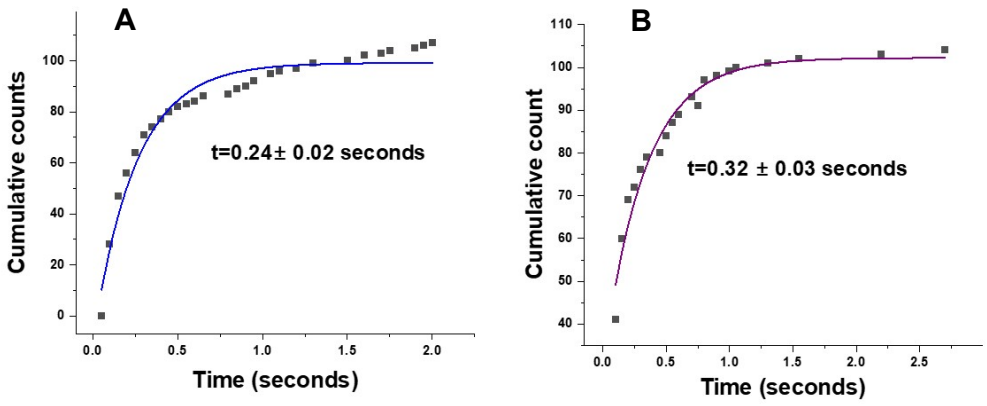

Supplementary Fig. 4. NSF disassembly assay at higher (50ms) resolution. A) Cumulated distribution showing average dwell time of the separated state present transiently before NStx-Cy3 disassembles (n=106 traces). **B**) Cumulated distribution showing average dwell time of the separated state present transiently before NSN25-Cy5 disassembles (n=103 traces).

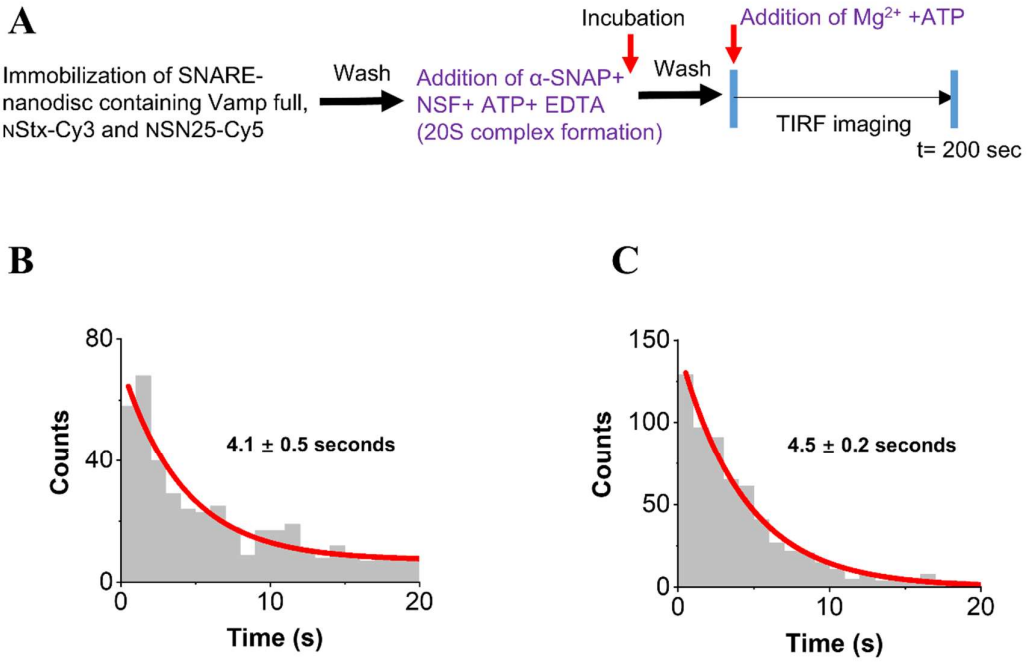

Supplementary Fig. 5. 20S complex disassembly. A) Procedure of the smFRET assay of 20S complex disassembly initiated by Mg^{2+} using TIRF microscope. **B**) A dwell time profile (NStx-Cy3) of the 20S complex disassembly upon the addition of Mg2+. Dwell time t=4.1±0.5 seconds (n=4 independent experiments) **C)** Dwell time profile (NStx-Cy3) of SNARE complex disassembly by NSF carried out using procedure 2A in parallel to S5B. Dwell time t=4.5±0.2 seconds (n=4 independent experiments).

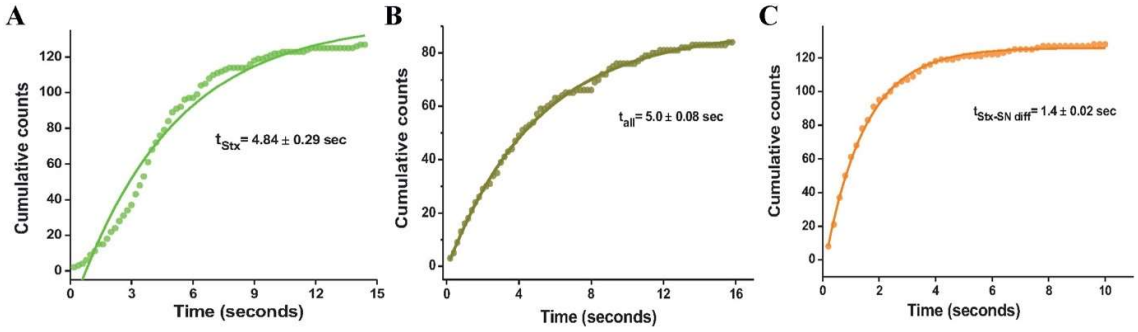

Supplementary Fig. 6. Vamp anchored SNARE disassembly by NSF monitored using three-colour single-molecule FRET. A) Cumulative distribution of latencies for the NStx-Cy3 leaving time (t_{Stx}) in pathway II, Fig. 3H. **B**) Cumulative distribution of latencies for the pathway I, Fig. 3H, where NStx and NSN25 disassemble together from Vamp (t_{all}). **C)** Cumulative distribution of the time difference between NStx and NSN25 disasembly (t_{diff}) in pathway II.

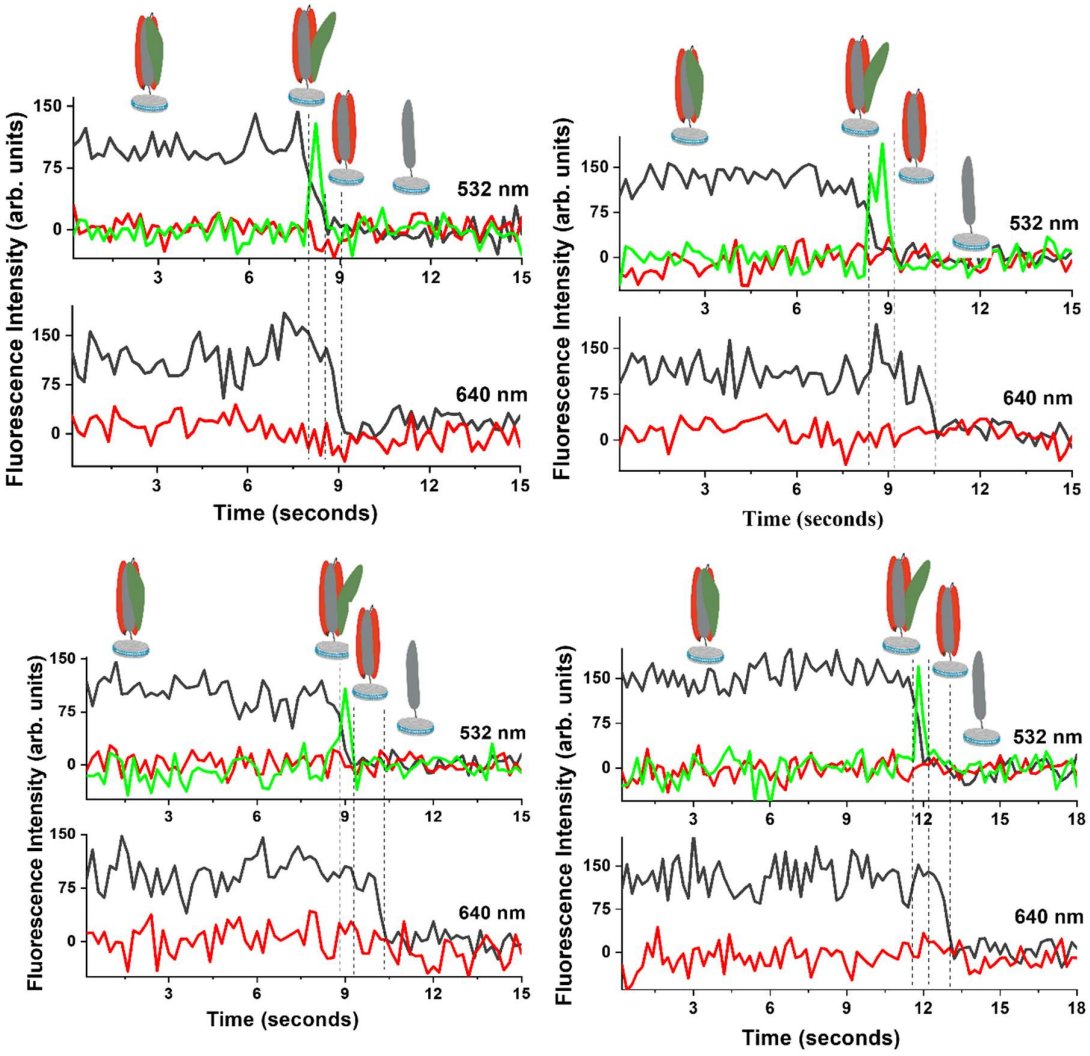

Supplementary Fig. 7. Vamp anchored SNARE disassembly by NSF monitored using three-colour single-molecule FRET. Real-time traces showing Vamp-anchored SNARE disassembly by NSF where NStx-Cy3 separation from the complex is observed before NStx disassembles first, followed by NSN-Cy5 (pathway II in Fig. 3H), along with the cartoon representation of the conformational states of SNARE complex.

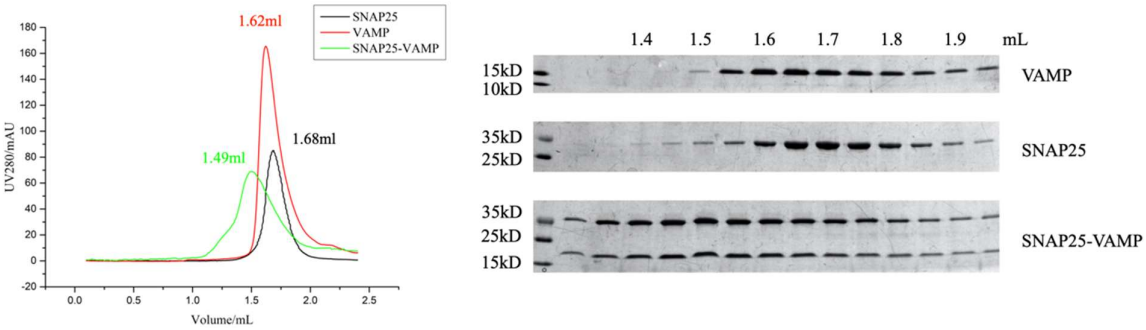

Supplementary Fig. 8. Vamp-SN25 binary complex formation verified by gel filtration chromatography (left panel) and SDS-PAGE corresponding to the peaks in the chromatogram (right panel).

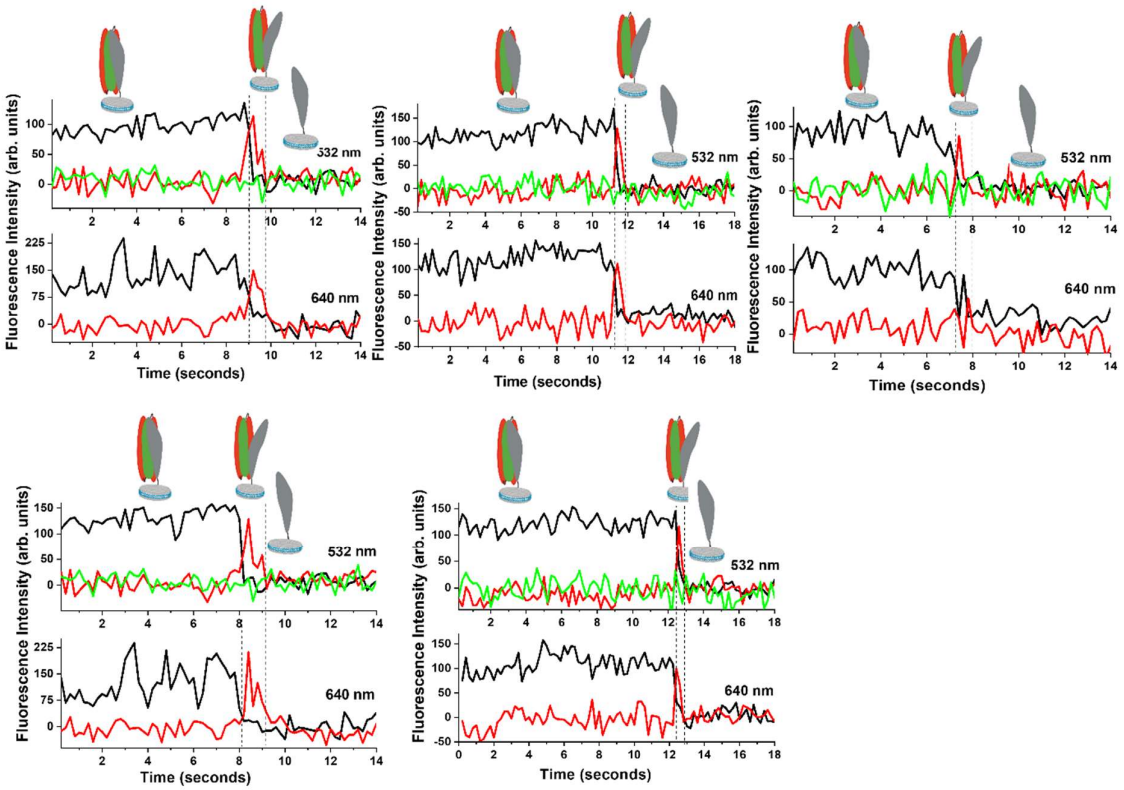

Supplementary Fig. 9. Syntaxin anchored SNARE disassembly by NSF monitored using three-colour single-molecule FRET. Real-time traces showing NStx-anchored SNARE disassembly by NSF, where a separation between NVamp-Cy3: NSN25-Cy5 from the NStx-Cy7 is observed before VAMP and NSN25 chains disassemble together from NStx (pathway II in Fig. 4I), along with the cartoon representation of the conformational states of SNARE complex.

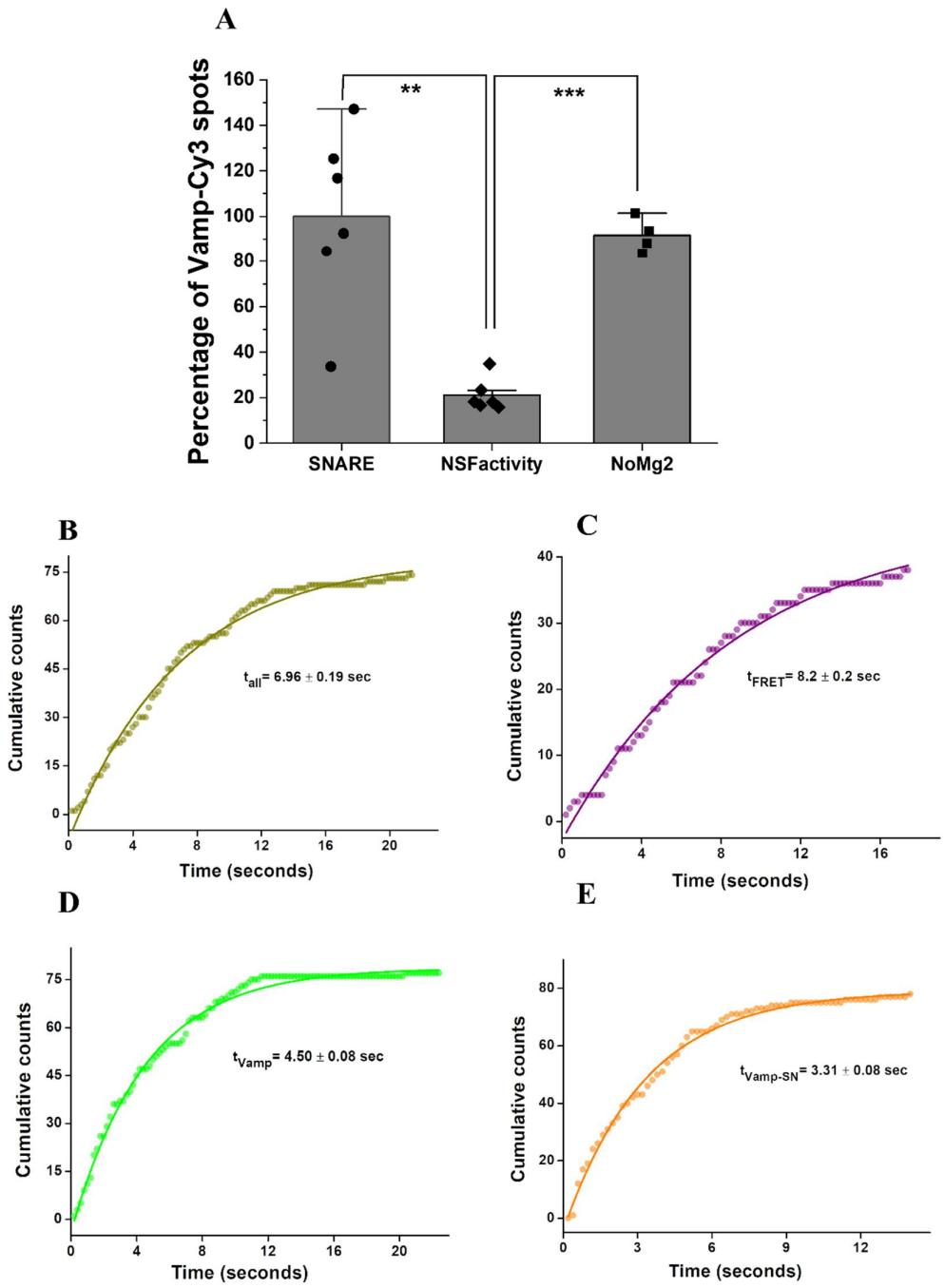

Supplementary Fig. 10. Syntaxin anchored SNARE disassembly by NSF monitored using three-colour single-molecule FRET. A) Number of NVamp-Cy3 spots detected in the Cy3 channel under various experimental conditions, *SNARE*; Stx-anchored SNARE containing NVamp-Cy3, NSN-Cy5 and NStx-Cy7 immobilized on the TIRFM surface, *NSF activity*; After

the addition of α-SNAP, NSF along with 2 mM ATP and 2 mM $MgCl_2$, *No* Mg^{2+}; After the addition of α-SNAP, NSF along with 2 mM ATP, without $MgCl_2$.) (n=6, independent SNARE disassembly experiments, p= ***<0.005 and **<0.01, two-sided paired t-test.). **B**) Cumulative distribution of latencies for the pathway I, Fig. 4I, where VAMP and SN25 leave together from NStx (t_{all}). **C**) Cumulative distribution of latencies for the FRET towards Cy7 disappearing before both chains leave in pathway II, Fig. 4I (t_{FRET}). **D)** Cumulative distribution of NVamp-Cy3 leaving time after FRET disappearing in pathway III (t_{Vamp}). **E)** Cumulative distribution of the time difference between NVamp and NSN25 leaving in pathway III ($t_{Vamp-SN}$).

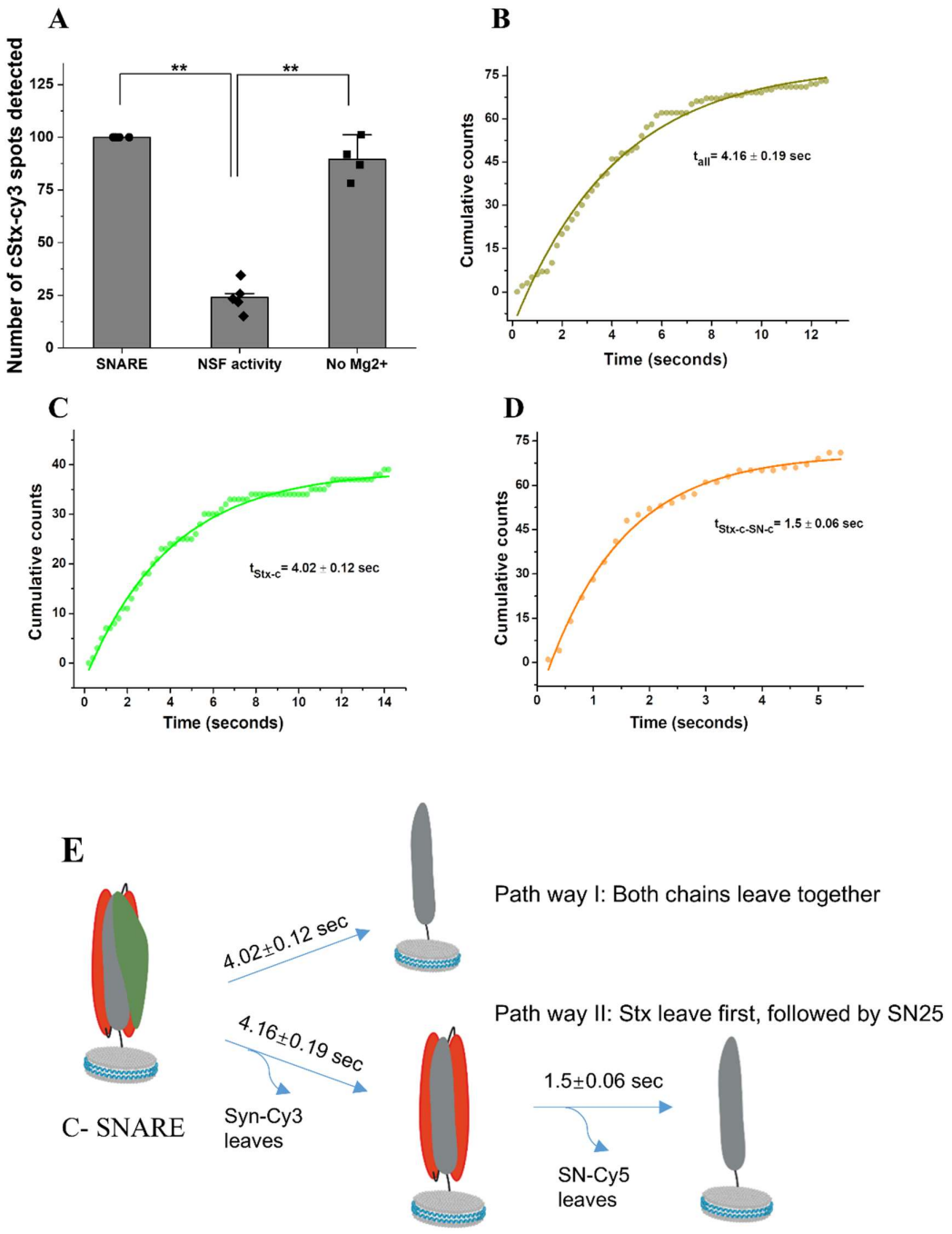

Supplementary Fig. 11. Vamp anchored C-SNARE disassembly by NSF monitored using three-colour single-molecule FRET. A) Number of cVamp-Cy3 spots detected in the Cy3 channel under various experimental conditions, *SNARE*; Vamp-anchored C-SNARE containing cStx-Cy3, cSN25-Cy5 and cVamp-Cy7 immobilized on the TIRFM surface, *NSF activity*; After the addition of α-SNAP, NSF along with 2 mM ATP and 2 mM $MgCl_2$, *No* Mg^{2+};

After the addition of α-SNAP, NSF along with 2 mM ATP, without $MgCl_2$.) (n=5-6, independent SNARE disassembly experiments, p= **<0.01, two-sided paired t-test.). **B**) Cumulative distribution of latencies for the pathway I shown in F, where cStx and cSN25 leave together from cVamp (t_{all}). **C**) Cumulative distribution of cStx-Cy3 leaving time in pathway II shown in F ($t_{Stx\text{-}c}$). **D)** Cumulative distribution of the time difference between cStx and cSN25 leaving ($t_{Stx\text{-}c\text{-}SN\text{-}c}$) in C-SNARE disassembly by NSF. **E**) Pictorial representation of two pathways of SNARE disassembly by NSF under our experimental design. Pathway I, showing cStx and cSN25 disassembly together from cVamp (42%) and Pathway II, where cStx disassembles first, followed by cSN (47%).

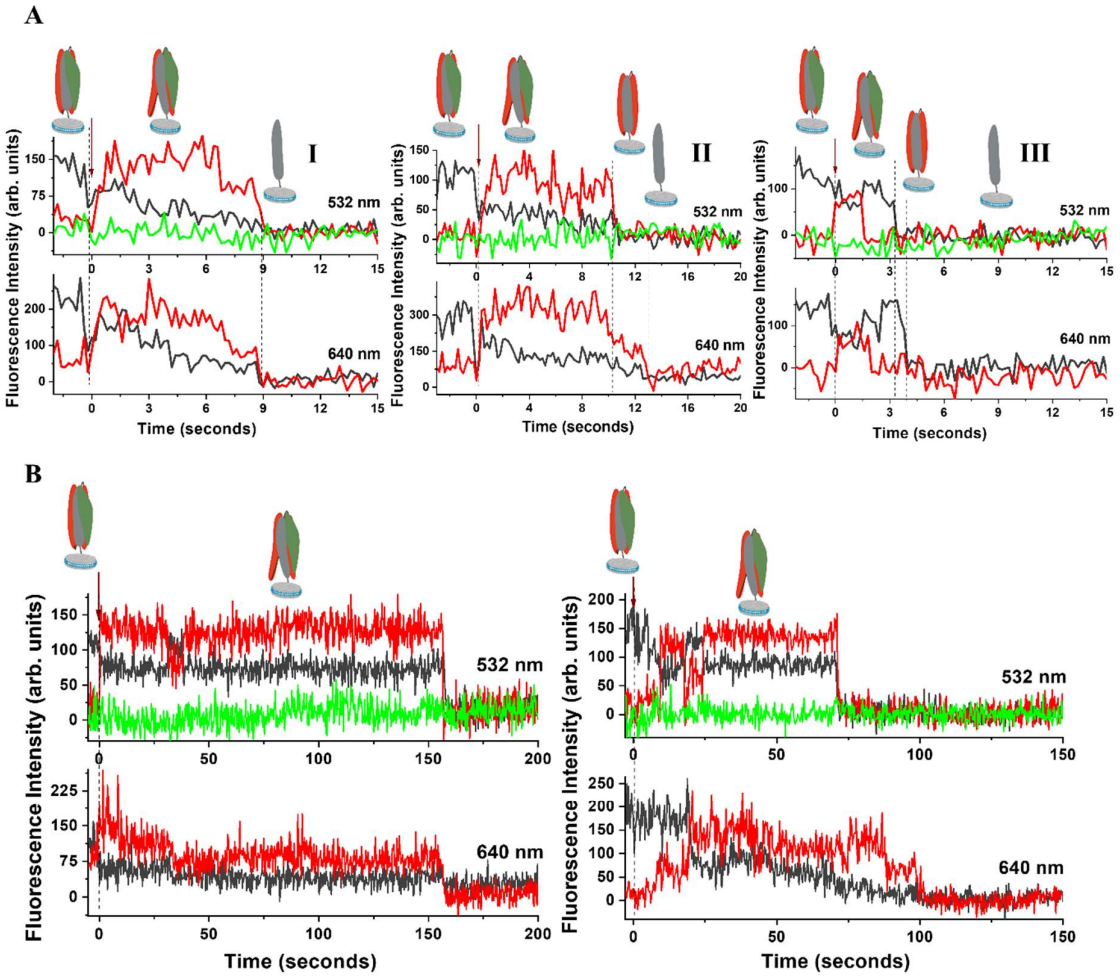

Supplementary Fig. 12. Vamp anchored C-SNARE-nanodisc disassembly by NSF monitored using three-colour single-molecule FRET. A) Real-time traces showing disassembly by NSF showing flexible nature at the C-terminal end of the Vamp-anchored C-SNARE during the disassembly with change in FRET. **B**) Real-time single-molecule traces showing change in intensity upon the addition of α-SNAP to the C-SNARE. Dotted line with arrow indicates the addition of α-SNAP.

A

Protein-Dye	Efficiency (%)
Vamp full-30C- Cy7	71
Vamp soluble 30C- Cy3	82
Vamp full-82C- Cy7	72
Syntaxin full-200C- Cy7	73
Syntaxin soluble-200C- Cy3	84
Syntaxin soluble-252C- Cy3	88
SNAP25-27C- Cy5	89
SNAP25-79C- Cy5	85

C

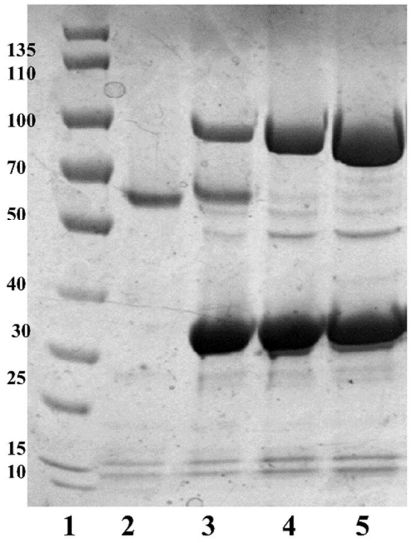

B

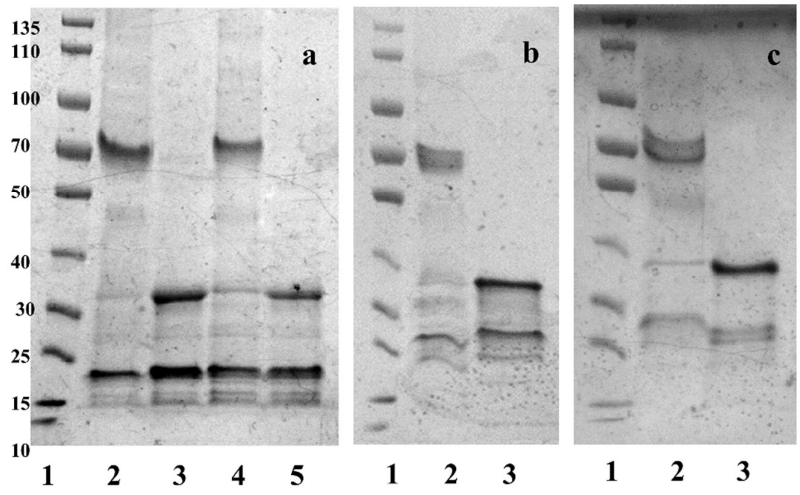

Supplementary Fig. 13: SNARE complex reconstitution and disassembly monitored using SDS-PAGE. (**A**) Labelling efficiency of SNARE proteins with the cyanine maleimide dyes. (**B**) SDS- PAGE gels showing- **a**) Marker (lane 1); Vamp-full SNARE at ~70kDa (lane 2); SNARE disassembly after the heating (lane 3); SNARE after urea wash (lane 4) and SNARE disassembly after the heating (lane 5), **b**) Marker (lane 1); Syntaxin-full SNARE after urea

wash (lane 2) and SNARE disassembly after the heating (lane 3), **c**) Marker (lane 1); Vamp-full C-SNARE after urea wash (lane 2) and SNARE disassembly after the heating (lane 3).

(**C**) SNARE disassembly by NSF. SDS- PAGE gels showing- Marker (lane 1), Vamp full SNARE (with His- tags removed) at ~70kDa (lane 2), SNARE in the presence of α-SNAP, NSF and ATP-EDTA (lane 3), SNARE in the presence of α-SNAP, NSF (2 μg), ATP and Mg^{2+} (lane 4), SNARE in the presence of α-SNAP, NSF (5 μg), ATP and Mg^{2+} (lane 5).

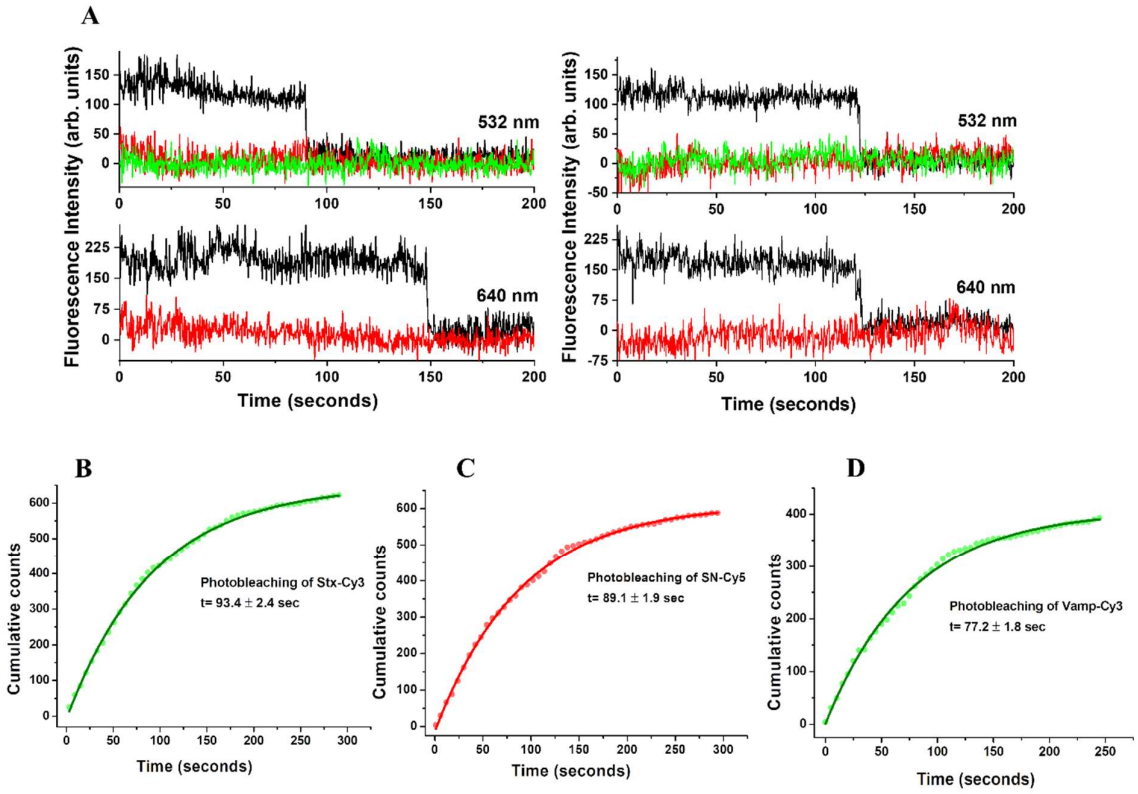

Supplementary Fig. 14. Photobleaching analysis of the three-colour SNARE complexes. **A**) Single-molecule trajectories of the NStx-Cy3 (green), NSN-Cy5 (red) and NVamp-Cy7 (grey) during photobleaching in the presence of oxygen scavenging buffer. **B-D**) Graphs showing cumulative distribution of latencies for the photobleaching of NStx-Cy3, NSN-Cy5 in Vamp anchored and NVamp-Cy3 in Syntaxin anchored SNARE complexes in the presence of oxygen scavenging buffer, respectively.

Supplementary Table 1: Amino acid sequences of the SNARE proteins used in the study.

All the mutations compared to the wild type are shown in red.

Protein	Sequence
Vamp full-30C	GSHMSATAATVPPAAPAGEGGPPAPPPNLTSN**C**RLQQTQAQVDEVVDIMR VNVDKVLERDQKLSELDDRADALQAGASQFETSAAKLKRKYWWKNLKMMII LGVI**S**AIILIIIIVYFST
Vamp full-82C	GSHMSATAATVPPAAPAGEGGPPAPPPNLTSNRRLQQTQAQVDEVVDIMR VNVDKVLERDQKLSELDDRADALQAGASQFETSA**C**KLKRKYWWKNLKMMI ILGVI**S**AIILIIIIVYFST
Vamp soluble-30C	GSHMSATAATVPPAAPAGEGGPPAPPPNLTSN**C**RLQQTQAQVDEVVDIMR VNVDKVLERDQKLSELDDRADALQAGASQFETSAAKLKRKYWWKNLK
Syntaxin full-200C	MKDRTQELRTAKDSDDDDDVTVTVDRDRFMDEFFEQVEEIRGFIDKIAENV EEVKRKHSAILASPNPDEKTKEELEELMSDIKKTANKVRSKLKSIEQSIEQEE GLNRSSADLRIRKTQHSTLSRKFVEVMSEYNATQSDYRER**S**KGRIQRQLEIT GRTTTSEELEDMLESGNPAIFASGIIMDSSISKQAL**C**EIETRHSEIIKLENSIRE LHDMFMDMAMLVESQGEMIDRIEYNVEHAVDYVERAVSDTKKAVKYQSKA RRKKIMIII**SS**VILGIIIASTIGGIFG
Syntaxin soluble-200C	MKDRTQELRTAKDSDDDDDVTVTVDRDRFMDEFFEQVEEIRGFIDKIAENV EEVKRKHSAILASPNPDEKTKEELEELMSDIKKTANKVRSKLKSIEQSIEQEE GLNRSSADLRIRKTQHSTLSRKFVEVMSEYNATQSDYRER**S**KGRIQRQLEIT GRTTTSEELEDMLESGNPAIFASGIIMDSSISKQAL**C**EIETRHSEIIKLENSIRE LHDMFMDMAMLVESQGEMIDRIEYNVEHAVDYVERAVSDTKK
Syntaxin soluble-252C	MKDRTQELRTAKDSDDDDDVTVTVDRDRFMDEFFEQVEEIRGFIDKIAENV EEVKRKHSAILASPNPDEKTKEELEELMSDIKKTANKVRSKLKSIEQSIEQEE GLNRSSADLRIRKTQHSTLSRKFVEVMSEYNATQSDYRER**S**KGRIQRQLEIT GRTTTSEELEDMLESGNPAIFASGIIMDSSISKQALSEIETRHSEIIKLENSIRE LHDMFMDMAMLVESQGEMIDRIEYNVEHAVDYVERAVSDT**C**KA
SNAP25-27C	GSHMASMTGGQQMGRGSEFMAEDADMRNELEEMQRRADQLADESL**C**ST RRMLQLVEESKDAGIRTLVMLDEQGEQLERIEEGMDQINKDMKEAEKNLTD LGKF**S**GL**S**V**S**P**S**NKLKSSDAYKKAWGNNQDGVVASQPARVVDEREQMAIS GGFIRRVTNDARENEMDENLEQVSGIIGNLRHMALDMGNEIDTQNRQIDRI MEKADSNKTRIDEANQRATKMLGSG
SNAP25-79C	GSHMASMTGGQQMGRGSEFMAEDADMRNELEEMQRRADQLADESLEST RRMLQLVEESKDAGIRTLVMLDEQGEQLERIEEGMDQINKDMKEAEKNL**C**D LGKF**S**GL**S**V**S**P**S**NKLKSSDAYKKAWGNNQDGVVASQPARVVDEREQMAIS GGFIRRVTNDARENEMDENLEQVSGIIGNLRHMALDMGNEIDTQNRQIDRI MEKADSNKTRIDEANQRATKMLGSG

Supplementary Table 2: Sequences of the primers used to generate desired protein mutants used in the study.

Primer name	Sequence
Stxsol C143S F	TACCGAGAACGCTCAAAAGGG
Stxsol C143S R	TCTTGCGAGTTTTCCCGCGTAG
Stxsol S200C F	GAGACCAGGCACTGTGAGATCAT
Stxsol S200C R	GGTCCGTGACACTCTAGTAGTTC
Stxsol- K252C F	CGTGTCTGACACCAAGTGTTGACTC
Stxsol- K252C R	ACACTTGGTGTCAGACACGGCCCTCT
pET28 C2S F	GAAATAATTTTCGTTAACTTTAAGAAGG
pET28 C2S R	CGAAAATTATTTCTAGAGGGGAA
SN25-T79C F	AAAGAATTTGTGCGACCTAGGAAA
SN25-T79C R	GCACAAATTCTTTTCTGCTTCTTTC
SN25 C27E F	ATGAGTCCCTGGAAAGCACCCGTCGCAT
SN25 C27E R	TTCCAGGGACTCATCAGCCAGCTGGTCA
SN25 E148C F	GAGATGGATTGTAACCTGGAGCAG
SN25 E148C R	ACAATCCATCTCATTTTCCCGGGCAT
SN25 C all S F	GAAAATTCTCCGGGCTTTCTGTGTCTCCCTCTAACAAGCTTAAA
SN25 C all S R	CTTGTTAGAGGGAGACACAGAAAGCCCGGAGAATTTTCCTAG
VAMP R30C F	ACCAGTAACTGCAGACTG
VAMP R30C R	TGCTGCAGTCTGCAGTTA
VAMPfull C103S F	TCTTGGGAGTGATTTCAGCCA
VAMPfull C103S R	GAGGATGATGGCTGAAATCAC
VAMP A82C F	AGTGCATGTAAGCTCAAGCGCA
VAMP A82C R	ACATGCACTTGTTTCAAACTGGG